Novel reinforcement of corrugated nanofiber tissue-engineered vascular graft to prevent aneurysm formation for arteriovenous shunts in an ovine model

Hiroshi Matsushita, MD,[a] Hidenori Hayashi, MD,[a] Katherine Nurminsky,[a] Tyler Dunn, BS,[a] Yusheng He, PhD,[a] Isaree Pitaktong, BS,[a] Yojiro Koda, MD,[a] Shanxiu Xu, BS,[a] Vivian Nguyen, BS,[a] Takahiro Inoue, MD,[a] Daniel Rodgers, BS,[a] Kevin Nelson, PhD,[b] Jed Johnson, PhD,[b] *and* Narutoshi Hibino, MD, PhD,[a] *Chicago, IL; and Hilliard, OH*

ABSTRACT

Objective: Many patients who require hemodialysis treatment will often require a prosthetic graft after multiple surgeries. However, the patency rate of grafts currently available commercially has not been satisfactory. Tissue engineering vascular grafts (TEVGs) are biodegradable scaffolds created to promote autologous cell proliferation and functional neotissue regeneration and, accordingly, have antithrombogenicity. Therefore, TEVGs can be an alternative prosthesis for small diameter grafts. However, owing to the limitations of the graft materials, most TEVGs are rigid and can easily kink when implanted in limited spaces, precluding future clinical application. Previously, we developed a novel corrugated nanofiber graft to prevent graft kinking. Reinforcement of these grafts to ensure their safety is required in a preclinical study. In the present study, three types of reinforcement were applied, and their effectiveness was examined using large animals.

Methods: In the present study, three different reinforcements for the graft composed of corrugated poly-ε-caprolactone (PCL) blended with poly(L-lactide-co-ε-caprolactone) (PLCL) created with electrospinning were evaluated: 1) a polydioxanone suture, 2) a 2-0 polypropylene suture, 3) a polyethylene terephthalate/polyurethane (PET/PU) outer layer, and PCL/PLCL as the control. These different grafts were then implanted in a U-shape between the carotid artery and jugular vein in seven ovine models for a total of 14 grafts during a 3-month period. In evaluating the different reinforcements, the main factors considered were cell proliferation and a lack of graft dilation, which were evaluated using ultrasound examinations and histologic and mechanical analysis.

Results: No kinking of the grafts occurred. Overall, re-endothelialization was observed in all the grafts at 3 months after surgery without graft rupture or calcification. The PCL/PLCL grafts and PCL/PLCL grafts with a polydioxanone suture showed high cell infiltration; however, they had become dilated 10 weeks after surgery. In contrast, the PCL/PLCL graft with the 2-0 suture and the PCL/PLCL graft covered with a PET/PU layer did not show any graft expansion. The PCL/PLCL graft covered with a PET/PU layer showed less cell infiltration than that of the PCL/PLCL graft.

Conclusions: Reinforcement is required to create grafts that can withstand arterial pressure. Reinforcement with suture materials has the potential to maintain cell infiltration into the graft, which could improve the neotissue formation of the graft. (JVS—Vascular Science 2022;3:182-91.)

Clinical relevance: In our basic science research study, we investigated tissue engineered vascular grafts for arteriovenous shunts. Our grafts were created with poly-ε-caprolactone and poly(L-lactide-co-ε-caprolactone) and designed with corrugated walls to avoid graft kinking. The grafts were implanted between the carotid artery and external jugular vein in a U-shape using an ovine model. To withstand the high pressure of blood on the arterial system, two types of reinforcement were applied to these tissue engineering vascular grafts. Because reinforcement of the graft could interfere with cell infiltration into the tissue engineering vascular grafts, the methods and material of reinforcement were investigated, in addition to the mechanical properties of the graft.

Keywords: Arteriovenous shunt; Corrugated nanofiber vascular graft; Large animal study; Smaller diameter prosthetic grafts; Tissue-engineered vascular grafts

From the Section of Cardiac Surgery, Biological Sciences Division, the University of Chicago, Chicago[a]; and Nanofiber Solutions, LLC, Hilliard.[b]

Research funding and the vascular grafts for the present study were provided by Nanofibersolutions (to N.H.).

Author conflict of interest: none.

Correspondence: Narutoshi Hibino, MD, PhD, Section of Cardiac Surgery, Biological Sciences Division, the University of Chicago, 5841 S Maryland Ave, Rm J652, MC5040, Chicago, IL 60637 (e-mail: nhibino@surgery.bsd.uchicago.edu).

The editors and reviewers of this article have no relevant financial relationships to disclose per the JVS-Vascular Science policy that requires reviewers to decline review of any manuscript for which they may have a conflict of interest.

2666-3503

https://doi.org/10.1016/j.jvssci.2022.01.002

The global estimated prevalence of chronic kidney disease is 13.4% (range, 11.7%-15.1%).[1] In 2017, 124,500 cases of end-stage renal disease (ESRD) were newly reported. Of the patients with incident ESRD, 86.9% had begun renal replacement therapy with hemodialysis (HD), 10.1% had started peritoneal dialysis, and 2.9% had undergone a preemptive kidney transplant. Patients treated with HD require creation of an arteriovenous fistula (AVF). These patients will often require multiple AVF operations and require prosthetic arteriovenous grafts for HD. A nationwide study performed in Japan in 1998 indicated that the prevalence of AVF creation was 4.8%; however, this proportion had increased to 7.1% by 2008.[2] The demand for vascular grafts for the AVF has been increasing. In general, the patency of synthetic grafts has remained low, with primary and secondary patency rates of the polytetrafluoroethylene (PTFE) graft at 1 year postoperatively reported as 43% and 64%, respectively.[3] A vascular graft with a high patency rate has been much anticipated by patients with ESRD, in part, because the low graft patency has been attributed to graft stenosis. Graft stenosis occurs most often at the graft—venous anastomosis and juxta-anastomotic venous segments and, less frequently, at the graft—arterial anastomosis.[4,5] This stenosis almost always arises from progressive neointimal hyperplasia. The cause of neointimal hyperplasia was analyzed in an in vivo study using large animals and thought to be due to a nonphysiologic inflammatory response resulting from graft bioincompatibility.[6]

TEVGs are composed of bioabsorbable materials, and the faster they are absorbed, the less of an inflammatory response results.[7] This has the potential to improve the issues with the currently commercially available grafts. Since Wystrychowski et al[8] first proposed the idea, several examples of TEVGs as arteriovenous grafts have been reported.[9,10] However, we have only reported studies conducted using large animal models with the acellular graft, which does not require cell seeding before grafting.[11,12] This method is low cost and can avoid the risk of infection associated with cell seeding.[13] In AVF surgery, the graft is often placed in a U-shape to produce many potential puncture sites. As described in our previous report, TEVGs can have low kink resistance, with stenosis resulting from graft kinking. To avoid this, a corrugated graft was created and reported.[11] One of the major remaining issues is potential graft dilation, because our previous study had had a short-term follow-up period, and the findings showed a tendency for graft expansion at the end of follow-up.[11]

In the present study, we reinforced the poly-ε-caprolactone (PCL)/poly(L-lactide-co-ε-caprolactone) (PLCL) grafts using several methods to determine the best method to prevent graft dilation and still allow for cell proliferation. We tested a biodegradable polydioxanone (PDO) suture, a nonbiodegradable 2-0 polypropylene suture, a polyurethane/polyethylene terephthalate (PET/PU) as an outer layer, and the PCL/PLCL graft alone as the control.

ARTICLE HIGHLIGHTS

- **Type of Research:** A single-center study of prospectively collected data
- **Key Findings:** Corrugated tissue-engineered vascular grafts reinforced by two different methods (suture reinforcement and extralayer reinforcement) implanted between the carotid artery and the external jugular vein in a sheep model (sheep, n = 7; grafts, n = 14) had an average patency rate of 57.1%, and re-endothelialization was observed 1 month after surgery without graft rupture, calcification, or aneurysmal changes.
- **Take Home Message:** The corrugated nanofiber graft reinforced with polypropylene suture successfully prevented aneurysm formation and maintained neotissue formation of the biodegradable graft because the space between sutures allowed the cells to infiltrate into the graft. We suggest that the reinforced corrugated tissue-engineered vascular graft could be a useful prosthetic graft for arteriovenous shunt procedures.

METHODS

Scaffold fabrication and suture additions. PLCL (6% w/w), PCL (6% w/w), and an 8/2 ratio of PU and PET (5% w/w) were dissolved separately in hexafluoroisopropanol. Each solution was mixed for ≥48 hours before electrospinning to ensure homogeneity. The PLCL and PCL solutions were simultaneously electrospun at a flow rate to yield a 1:1 mass ratio of PLCL/PCL. The solutions were electrospun with an applied voltage of +20 kV on the needle and −7 kV on the collector, such that a stable Taylor cone was established. Each polymer solution was electrospun onto a cylindrical mandrel rotating at 150 rpm with an outer diameter of 6 mm until the fiber deposition had generated a vascular scaffold with a wall thickness of 400 μm ± 10%. The inner diameter of the graft was designed to be 5 mm, with a length of 5 cm.

For the grafts reinforced with PET/PU, the PET/PU solution was electrospun on the collector until a final wall thickness of 800 μm ± 10% had been achieved. The electrospun scaffold was then removed from the mandrel and corrugated with a medical grade monofilament to improve the kinking radius and maneuverability.

For the grafts reinforced with suture, the helical suture structure was placed over the 400 μm ± 10% scaffold, and electrospinning of the PCL and PLCL material was continued until a final wall thickness of 800 μm ± 10% was achieved (Fig 1, *A*). No corrugation was necessary because the helical suture structure provided kinking

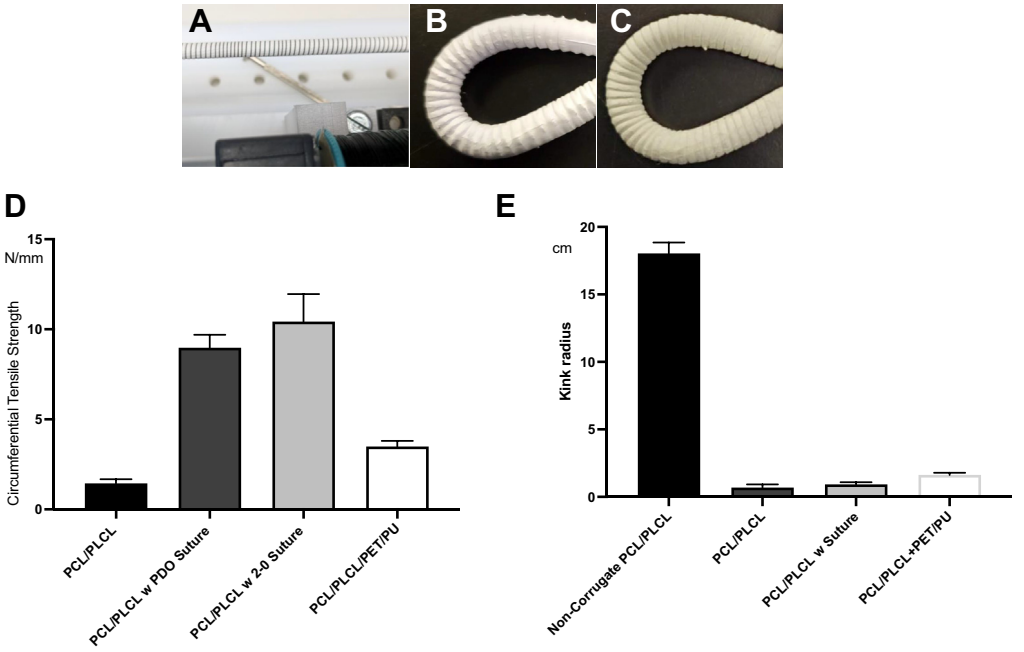

Fig 1. A, Photograph showing reinforcement with a suture. **B,** Poly-ε-caprolactone *(PCL)* blended with poly(L-lactide-co-ε-caprolactone) *(PLCL)* graft. **C,** PCL/PLCL graft reinforced with polyethylene terephthalate/polyurethane (PET/PU) layer. Comparison of circumferential tensile strength **(D)** and kink radius **(E)** for the PCL/PLCL graft, PCL/PLCL graft with a polydioxanone *(PDO)* suture, PCL/PLCL graft with a 2-0 suture, and PCL/PLCL covered with a PET/PU monolayer.

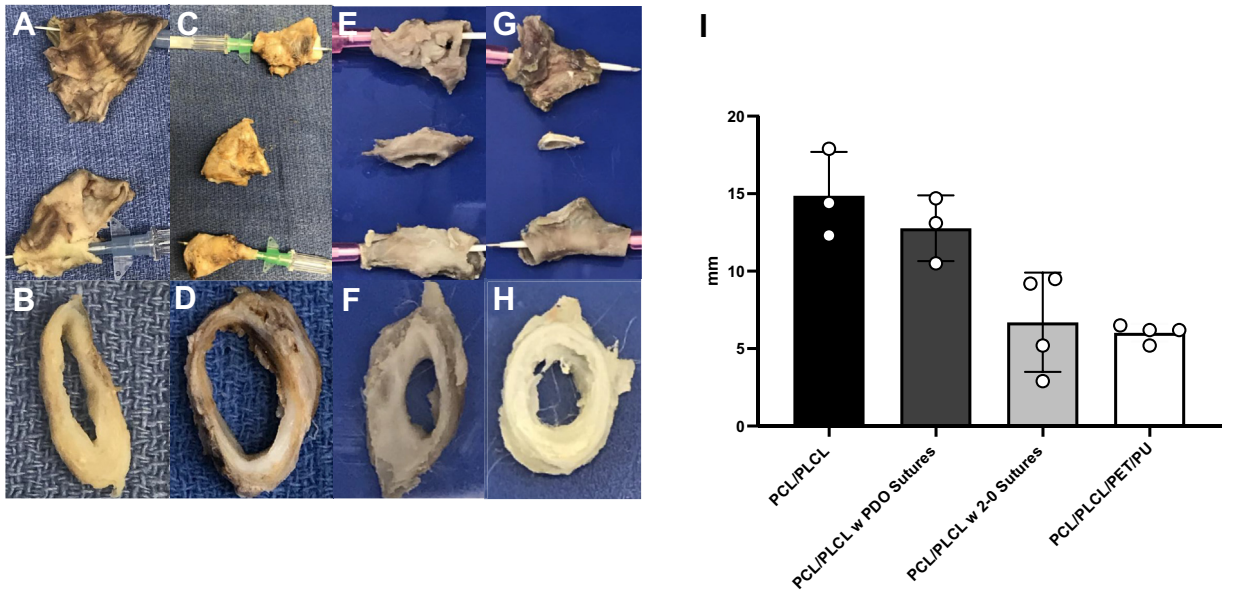

Fig 2. Macroscopic images of tissue engineering vascular grafts (TEVGs) and arterial and venous anastomosis sites and cross-sectional images of the TEVGs. **A, and B,** Poly-ε-caprolactone/poly(L-lactide-co-ε-caprolactone) *(PCL/PLCL).* **C,D,** PCL/PLCL with a polydioxanone *(PDO)* suture. **E, and F,** PCL/PLCL with a 2-0 suture. **G, and H,** PCL/PLCL covered with a polyethylene terephthalate/polyurethane *(PET/PU)* monolayer. **I,** Inner diameters measured microscopically.

resistance and maneuverability. The original wall thickness of the PET/PU (800 μm) was larger than that of the PCL/PLCL (400 μm) owing to the different reinforcement method used.

Mechanical testing. The grafts (at both time 0 and explanted) were tested for circumferential tensile strength in accordance with the International Organization for Standardization 7198:2016 guidelines. In brief,

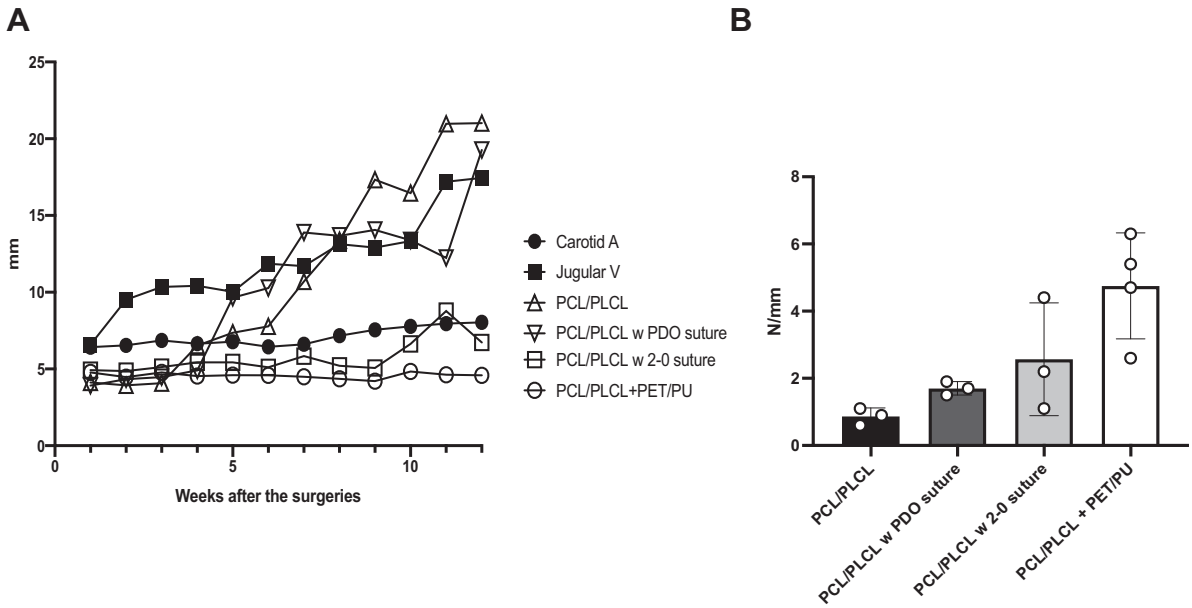

Fig 3. A, Inner diameter of grafts measured using serial ultrasound examinations of the tissue engineering vascular grafts (TEVGs) from 1 to 12 weeks after surgery. **B,** Circumferential tensile strength measured after graft explantation. *A,* Artery; *PCL/PLCL,* poly-ε-caprolactone/poly(L-lactide-co-ε-caprolactone); *PDO,* polydioxanone; *PET/PU,* polyethylene terephthalate/polyurethane; *V,* vein; *w,* with.

the grafts were stretched at 50 mm/min until a break was detected by the software. The circumferential tensile strength was defined as the maximum load divided by twice the sample length.

Kink testing was completed using the method as described in International Organization for Standardization 7198:2016 guidelines for kink diameter and radius (A.5.8). In brief, a cylindrical mandrel was used to determine the kink radius. This was accomplished by forming a loop with the test sample and pulling the ends of the sample in opposite directions to reduce the loop until a kink was observed. The appropriately sized cylindrical mandrel was placed within the loop to measure the kink diameter, and the mandrel size was recorded.

Graft implantation. The Animal Care and Use Committee at Q-Test Laboratories (Columbus, Ohio) approved the care, use, and monitoring of animals for the sheep experiments. Fourteen custom-made nanofiber TEVGs were implanted bilaterally as arteriovenous shunts between the common carotid artery to the ipsilateral external jugular vein in seven sheep. Implantation was accomplished as previously described.[12] In brief, all sheep were anesthetized with 1% to 2% isoflurane and positioned in the dorsal recumbency during surgery. Heparin (100 IU/kg) was administrated intravenously after exposure of the bilateral common carotid artery and external jugular vein. An end-to-side vascular anastomosis was performed with a 5-cm graft and a 7-0 Prolene (Ethicon, Inc, Raritan, NJ) suture in the same fashion as described previously.[11] Hemostasis was obtained, and the muscle, subcutaneous tissue, and dermal incision layers were closed. Antibiotic treatment (cefazolin) was administrated intraoperatively and for 7 days postoperatively. All the sheep were maintained with a daily oral dose of aspirin (325 mg/d) until the end of the study. Serial color Doppler ultrasound examinations were performed to estimate graft patency and measure the lumen diameter and blood flow velocity. The sheep were euthanized using pentobarbital sodium 12 weeks after implantation.

Ultrasound examination. Color Doppler ultrasound was performed every week after implantation to determine graft patency according to the lumen diameter of the TEVG. Both the anastomosis site and the middle of the grafts were measured. If blood flow was observed at all the sites, the graft was determined to be patent. Ultrasound images were assembled using a Philips HD11 XE ultrasound machine and a probe of adequate frequency (model no. L15-7io; Philips, Amsterdam, Netherlands) to assess the vascular structures.

Histologic and immunohistochemistry examinations. The middle parts of the explanted TEVG samples were fixed in 10% formalin for 24 hours at 4°C and then embedded in paraffin for standard histologic analysis with hematoxylin and eosin, Masson's trichrome, Verhoeff-van Gieson, and von Kossa staining. For immunohistochemistry, the tissue sections were deparaffinized, rehydrated, and blocked for endogenous peroxidase activity and nonspecific staining. The primary antibodies used included von Willebrand factor (1:2000;

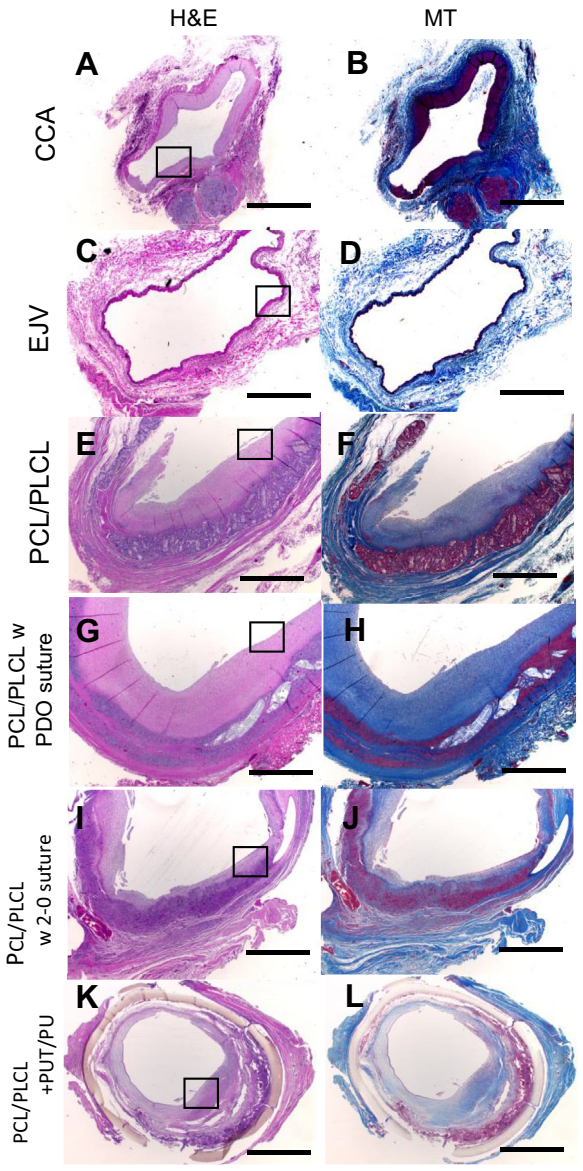

Fig 4. Histologic analysis of tissue engineering vascular grafts (TEVGs). Hematoxylin and eosin (H&E) stain **(A, C, E, G, I, and K)** and Masson's trichrome (MT) stain **(B, D, F, H, J, and L)**. Original magnification ×1.25. Scale bar = 2 mm. *CCA,* Common carotid artery; *EJV,* external jugular vein; *PCL/PLCL,* poly-ε-caprolactone/poly(L-lactide-co-ε-caprolactone); *PDO,* polydioxanone; *PET/PU,* polyethylene terephthalate/polyurethane; *w,* with.

Dako, Agilent Technologies, Santa Clara, Calif), α-smooth muscle actin (α-SMA; 1:500; Dako), and CD68 (1:200; Abcam, Cambridge, UK). Biotinylated secondary antibodies and horseradish peroxidase bound with streptavidin were then used before the color development of the chromogenic reaction with 3,3-diaminobenzidine (Vector Laboratories, Burlingame, Calif). Nuclei counterstaining was performed using Gill's hematoxylin (Vector Laboratories). The number of cells was measured by magnifying the number of nuclei under hematoxylin and eosin staining and the number of α-SMA–positive cells under immunohistochemical staining 20-fold from the intima to the tunica media tissue. The four samples were then averaged.

Statistical analysis. For all experiments, the data are presented as the mean ± standard deviation.

RESULTS

Graft morphology. The PCL/PLCL grafts (Fig 1, *B*), PCL/PLCL grafts covered with a PET/PU layer (Fig 1, *C*), and PCL/PLCL grafts with a suture could be bent 180° without kinking because of the corrugation.

Mechanical properties of preimplanted grafts. The circumferential tensile strength of the implanted PCL/PLCL graft (1.444 ± 0.224 N/mm) was lower than that of the reinforced grafts. Among the reinforced TEVGs, the PCL/PLCL graft with a 2-0 suture was the strongest (10.433 ± 1.520 N/mm), followed by the PCL/PLCL graft with a PDO suture (8.977 ± 0.715 N/mm). The PCL/PLCL graft covered with a PET/PU layer was stronger than the PCL/PLCL graft (3.496 ± 0.304 N/mm) but less than that of the other two reinforced groups (Fig 1, *D*). The original wall thickness of the reinforced TEVGs (800 μm) was larger than that of the PCL/PLCL graft (400 μm) resulting from the different reinforcement methods. The kink radius of the corrugated PCL/PLCL graft (1.633 ± 0.152 cm) was less than that of the noncorrugated PCL/PLCL graft (18.033 ± 0.802 cm). No differences were found in the kink radius among the reinforced grafts (PCL/PLCL graft reinforced with suture, 0.933 ± 0.153 cm; PCL/PLCL graft covered with a PET/PU layer, 1.633 ± 0.153 cm; Fig 1, *E*).

Graft assessment after explantation. All seven sheep survived postoperatively. Because of difficulty in evaluating graft patency over time using ultrasound, we evaluated the patency using direct measurement of the explanted grafts (Fig 2, *A-H*). No graft obstruction was found in the PCL/PLCL grafts without reinforcement. The average graft patency rate of the PCL/PLCL graft with a 2-0 suture and the PCL/PLCL graft covered with a PET/PU layer was 50% (two of four grafts) and that of the PCL/PLCL graft with a PDO suture was 33.3% (one of three grafts). The inner diameter measured microscopically in the explanted TEVGs was smallest for the PCL/PLCL graft covered with a PET/PU layer (6.025 ± 0.568 mm), followed by the PCL/PLCL graft with a 2-0 suture (6.700 ± 3.203 mm) and the PCL/PLCL graft with a PDO suture (12.767 ± 2.120 mm). In contrast, the PCL/PLCL grafts had the largest diameter (14.867 ± 2.829 mm; Fig 2, *I*).

Serial ultrasound examinations. The sheep were observed for 12 weeks postoperatively. At 6 weeks after surgery, the PCL/PLCL graft and PCL/PLCL graft with a

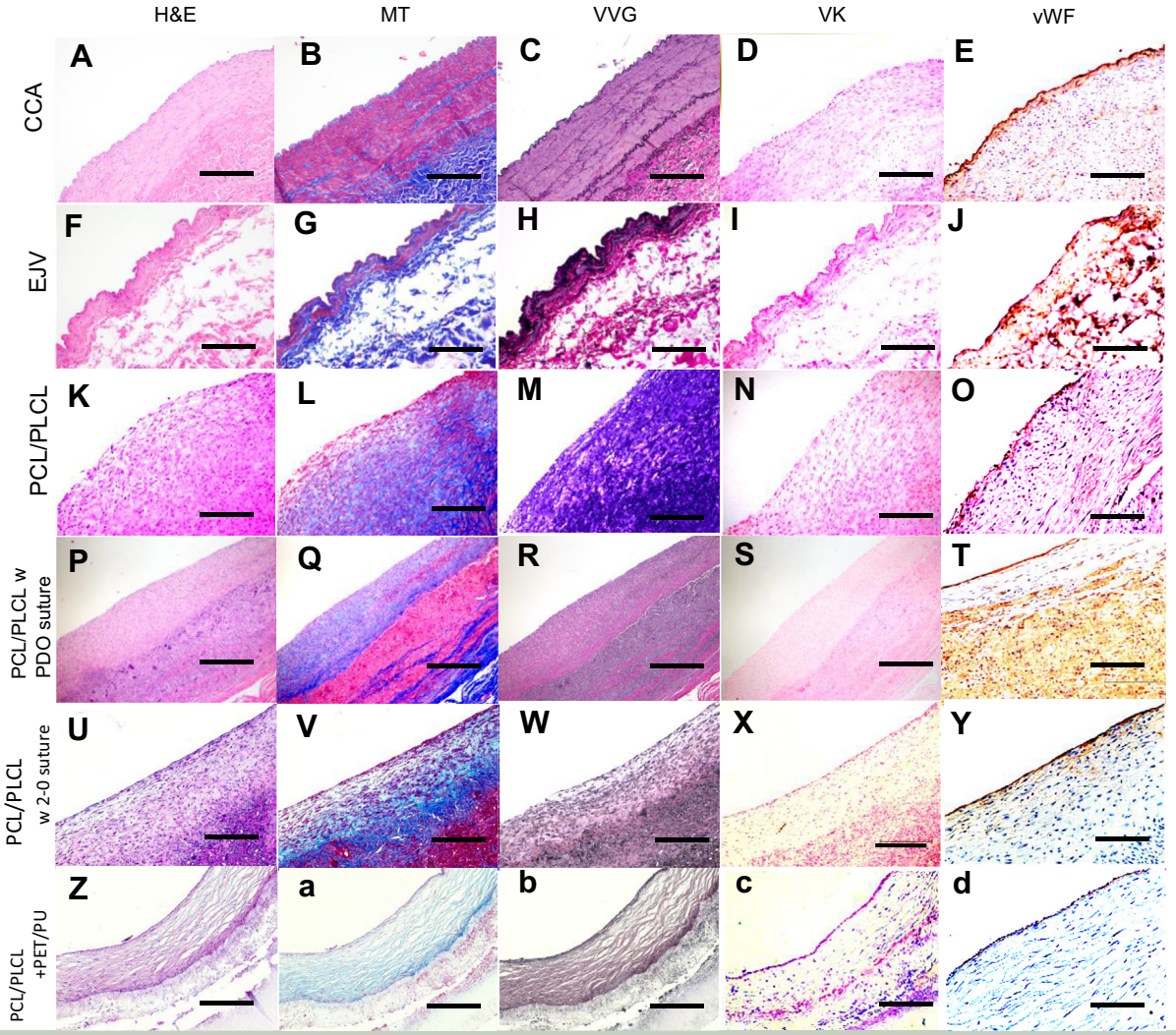

Fig 5. Histologic analysis of tissue-engineered vascular grafts (TEVGs), common carotid artery (*CCA*) and external jugular vein (*EJV*) 12 weeks after surgery. Hematoxylin and eosin (H&E) staining **(A, F, K, P, U, and Z)**, Masson's trichrome (MT) staining **(B, G, L, Q, V, and a)**, Verhoeff-van Gieson (VVG) stain **(C, H, M, R, W, and b)**, von Kossa (VK) staining **(D, I, N, S, X, and c)**, von Willebrand factor (vWF) immunostaining **(E, J, O, T, Y, and d)**: 10× magnification for H&E, MT, VVG, and VK staining; 20× magnification for vWF and α-SMA staining. Scale bar = 350 μm for ×10 magnification. Scale bar = 150 μm for ×20 magnification. *PCL/PLCL,* Poly-ε-caprolactone/poly (L-lactide-co-ε-caprolactone); *PDO,* polydioxanone; *PET/PU,* polyethylene terephthalate/polyurethane; *w,* with.

PDO suture showed a tendency toward an increased lumen diameter. The diameters were approximately consistent with the jugular vein's degree of enlargement. However, the PCL/PLCL graft with a 2-0 suture and the PCL/PLCL graft covered with a PET/PU layer did not show a clear increasing trend (Fig 3, *A*).

Mechanical properties of the explanted grafts. The circumferential tensile strength of the explanted PCL/PLCL covered with a PET/PU layer (4.606 ± 1.550 N) was greater than that of the PCL/PLCL graft (0.867 ± 0.252 N), PCL/PLCL graft with a PDO suture (1.700 ± 0.200 N), and PCL/PLCL graft with a 2-0 suture (2.567 ± 1.680 N; Fig 3, *B*).

Histologic analysis of the TEVG. The results from the histologic and immunohistochemistry analyses are presented in Figs 4 to 6. In all the grafts, no apparent calcified tissue was seen with von Kossa staining (Fig 5, *D, I, N, S, X, and c*). Elastin enhancement was observed with Verhoeff-van Gieson staining (Fig 5, *C, H, M, R, W, and b*). A single cell layer positive for von Willebrand factor was observed with von Willebrand factor staining (Fig 5, *E, J, O, T, Y, and d*). The number of cells found on hematoxylin and eosin staining in 20× magnification images was lower for the PCL/PLCL graft covered with a PET/PU layer (560.0 ± 180.6) than for the PCL/PLCL graft (1258.3 ± 63.3; Fig 7, *A*). However, no apparent difference was found in the number of α-SMA–positive cells (Fig 7, *B*).

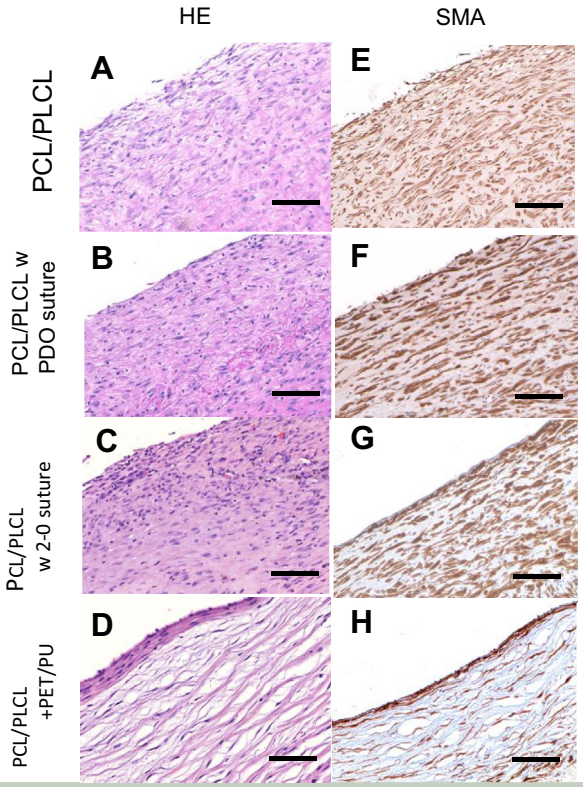

Fig 6. Immunohistochemistry of tissue-engineered vascular grafts (TEVGs). Hematoxylin and eosin *(HE)* staining (**A-D**) and α-smooth muscle actin (*SMA*) staining (**E-H**). Original magnification ×20; scale bar = 150 μm. *PCL/PLCL,* Poly-ε-caprolactone/poly(L-lactide-co-ε-caprolactone); *PDO,* polydioxanone; *PET/PU,* polyethylene terephthalate/polyurethane; *w,* with.

DISCUSSION

At present, the commercially available small-diameter arterial grafts often do not provide adequate patency after AVF creation. The use of TEVGs has the potential to solve this problem. When a prosthetic graft is used in arteriovenous shunt surgery, it is often implanted in a U-shape[14]; however, the TEVGs often have a low kink resistance, which can cause graft occlusion. Therefore, we previously created a high kink resistant TEVG and studied its effects using large animals. Our previous study had short-term follow-up and the grafts had shown a tendency for graft expansion at the end of the follow-up period.[11] In the present study, we added reinforcements to the graft and for a longer follow-up period. When we began to reinforce the PCL/PLCL graft, a concern was expressed regarding the effects grafting would have on kink resistance. However, we found little differences between all groups.

In previous studies of carotid graft implantation in a pig model, the reported graft patency was 60% to 80%.[15] Our results showed a lower patency of 50% to 70% because the graft was implanted in a U-shape in our study. In contrast, other studies had used a straight graft. The U-shape implantation would have caused higher wall shear stress, which would eventually lead to lower patency in our model compared with others.

Many researchers have worked to reinforce acellular grafts to make them more resistant to high-pressure circulation. At the in vitro level, numerous possibilities have been explored in recent years, including bilayer scaffolds of a PCL—collagen blend,[16] a bilayer scaffold of an aligned fibrous poly(lactic acid) outer layer with a randomly oriented elastic PCL inner layer scaffold,[16] PCL/collagen and PCL/silica bilayers,[17] and silk-fibroin/polyurethane three-layer scaffold.[18] In addition, many in vivo studies using small animals have been reported.[19–23] However, when we studied reports of small diameter grafts using large animals, the number of studies was significantly smaller. Izhar et al[24] reported that 6-mm-diameter elastomeric poly(ether urethane) scaffolds coated with poly(ethylene glycol)/poly(lactic acid) block copolymer were implanted in the carotid artery of mongrel dogs and evaluated after 12 weeks. No apparent thrombus formation or dilatation was observed.[24] Guang et al[25] reported that 2.5-mm-diameter, 4-cm-long, double-layer composite grafts of heparin-conjugated polycaprolactone and PU—collagen type I were implanted into the femoral artery of Beagle dogs showed no apparent stenosis or dilatation at 8 weeks after surgery. Both studies had used a combination of bioabsorbable and nonabsorbable materials.[24,25] Therefore, although differences were found in the experimental systems used, considering the results of our experiments against those of the cited studies, we believe the use of nonbioabsorbable materials is necessary to withstand the arterial pressure.

In the present study, extended graft diameters were observed in the PCL/PLCL and PCL/PLCL with PDO grafts. It is common for the shunt vein diameter of mature AVFs to dilate by 4 to 7 mm, and it is necessary to consider whether this dilation is a pathologic dilation.[26]

Significant venous dilation of AVFs can be diagnosed as aneurysms of the AVF and can require surgical intervention. However, the exact definition of aneurysms of AVFs has not yet been established, and the criteria have varied from study to study, such as a venous diameter more than three times the diameter of the adjacent veins and >2 cm or an enlargement of all three vessel layers with a diameter >18 mm or approximately three times the diameter of the outflow vein of a mature AVF.[26,27] Thus, the PCL/PLCL graft and PCL/PLCL graft with a PDO suture could be considered pathologic extensions. In contrast, the PCL/PLCL graft with a 2-0 suture and PCL/PLCL graft covered with a PET/PU layer were judged to be within the normal range. To discuss the causes of TEVG enlargement, it is necessary to consider the pathogenesis of shunt aneurysms in the arteriovenous shunt. The degradation of elastin, collagen, and other constituents of the arterial extracellular matrix has been thought to be the cause. These are mediated by angiotensin II,

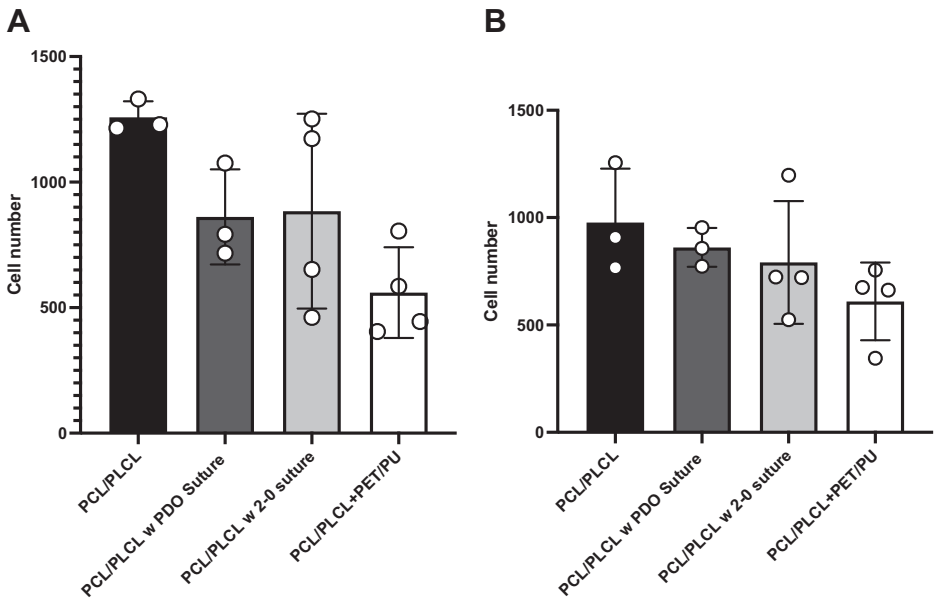

Fig 7. A, Graph showing number of nuclei counted on hematoxylin and eosin stain. **B,** Graph showing area of smooth muscle actin (SMA)—positive cells counted on SMA stain. Original magnification ×20 for both. *PCL/PLCL,* Poly-ε-caprolactone/poly(L-lactide-co-ε-caprolactone); *PDO,* polydioxanone; *PET/PU,* polyethylene terephthalate/polyurethane; *w,* with.

Table. Characteristics of each tissue-engineered vascular graft (TEVG)

TEVG	Resistance to expansion[a]	Cell infiltration[b]
PCL/PLCL	+	+++
PCL/PLCL with PDO	++	++
PCL/PLCL with 2-0 suture	+++	++
PCL/PLCL with PET/PU layer	+++	+

PCL/PLCL, Poly-ε-caprolactone/poly(L-lactide-co-ε-caprolactone); *PDO,* polydioxanone; *PET/PU,* polyethylene terephthalate/polyurethane.
[a]Resistance to expansion: ++, expansion >5 mm but <10 mm; +, expansion >10 mm but <20 mm; +, expansion >20 mm.
[b]Cell infiltration: ++, number of cells >1000; +, number of cells >750 but <1000; +, number of cells, ≥0 but <750.

transforming growth factor-β signaling, and inflammation. Matrix metalloproteinases (MMPs), which are produced by vascular smooth muscle cells and inflammatory cells, are upregulated in the walls of aneurysms and seem central to the pathogenesis of aneurysm formation.[28-30] Tara et al[31] reported that when PLCL scaffolds reinforced by polylactic acid were implanted into the abdominal aorta of mice, the precedent was aneurysmal dilatation, and the gene expression of MMP-9 and Itgam, a marker for macrophages, was upregulated.[31] We suggest that activation of MMPs could have occurred in our study, in addition to inadequate formation of the arterial extracellular matrix.

The requirements for tissue engineering vascular graft material include matched mechanical properties, blood compatibility, endothelium friendliness, and biodegradability.[32] Many studies have emphasized the importance of biodegradability.[8,33,34] In a study of rats, bioabsorbable and nonabsorbable materials were seen as patches in the right ventricular outflow tract.[34] The nonabsorbable, expanded PTFE patch showed deposition of endothelial cells and collagen only on the surface, without cellular infiltration into the material. Patches with polyglycolic acid and a co-polymer of ε-caprolactone and L-lactic acid reinforced with poly-L-lactide showed good cell infiltration.[34] Therefore, the PET/PU layer, which is a nonabsorbable material, appears to inhibit cell invasion. Long-term persistence of materials will result in a nonphysiologic inflammatory response.[8] The development of anastomotic stenosis in PTFE grafts has been thought to result from this inflammatory response.[35] The accumulation of T lymphocytes in this inflammatory response has been confirmed, and it has been reported that the release of interferon-γ inhibits smooth muscle cells and fibroblast proliferation.[36,37] Although PDO and 2-0 polypropylene reinforcements are not dense and might not mechanically inhibit cell invasion, these inflammatory responses could inhibit cell invasion.

The grades of resistance of the reinforced grafts to expansion and cell infiltration are presented in the

Table. The replacement of TEVGs with autologous tissue through cellular infiltration is of paramount importance, because the mechanically stronger grafts with reinforcement tend to be less invasive. However, the mechanical properties of the graft in adapting to the high-pressure AVF shunt ensures the safety of the graft. Our data have shown that the two are incompatible. Therefore, the balance between the two and the mechanical properties required by the circulatory system to be transplanted should be fully considered when adapting the graft for application.

The present study had some limitations. These included the small number of large animals used, and the limited number of samples, although the grafts were implanted bilaterally. Furthermore, the follow-up period was short. In addition, the hemodynamics of the grafts transplanted between the carotid artery and vein in sheep could differ from the hemodynamics between the arteriovenous veins in the forearm of AVFs performed in humans.

CONCLUSIONS

The PCL/PLCL graft is an ideal material for TEVGs because it promotes positive cell invasion. However, implantation into the arterial system can lead to a trend toward diameter expansion in the long term. Reinforcement with suture materials has the potential to maintain cell infiltration into the graft, which could improve the neotissue formation of the graft.

The vascular grafts used in the present study were provided by Nanofibersolutoins.

AUTHOR CONTRIBUTIONS

Conception and design: HM, HH, KN, TD, YH, IP, YK, SX, VN, TI, DR, KN, JJ, NH

Analysis and interpretation: HM, HH, KN, TD, YH, IP, YK, SX, VN, TI, DR, KN, JJ, NH

Data collection: HM, HH, KN, TD, YH, IP, YK, SX, VN, TI, DR, KN, JJ, NH

Writing the article: HM, HH, KN, TD, YH, IP, YK, SX, VN, TI, DR, KN, JJ, NH

Critical revision of the article: HM, HH, KN, TD, YH, IP, YK, SX, VN, TI, DR, KN, JJ, NH

Final approval of the article: HM, HH, KN, TD, YH, IP, YK, SX, VN, TI, DR, KN, JJ, NH

Statistical analysis: Not applicable

Obtained funding: Not applicable

Overall responsibility: HM

REFERENCES

1. Lv J-C, Zhang L-X. Prevalence and disease burden of chronic kidney disease. Adv Exp Med Biol 2019;1165:3-15.
2. Hatakeyama T, Okamoto H, Nakazawa T, Nonaka T, Sasaki S, Hoshino M. Introduction of arteriovenous grafts with graft insertion anastomosis for hemodialysis access. J Vasc Surg 2017;66:952-7.
3. Cinat ME, Hopkins J, Wilson SE. A prospective evaluation of PTFE graft patency and surveillance techniques in hemodialysis access. Ann Vasc Surg 1999;13:191-8.
4. Asif A, Gadalean FN, Merrill D, Cherla G, Cipleu CD, Epstein DL, et al. Inflow stenosis in arteriovenous fistulas and grafts: a multicenter, prospective study. Kidney Int 2005;67:1986-92.
5. Kanterman RY, Vesely TM, Pilgram TK, Guy BW, Windus DW, Picus D. Dialysis access grafts: anatomic location of venous stenosis and results of angioplasty. Radiology 1995;195:135-9.
6. Li L, Terry CM, Shiu Y-TE, Cheung AK. Neointimal hyperplasia associated with synthetic hemodialysis grafts. Kidney Int 2008;74:1247-61.
7. Wu W, Allen RA, Wang Y. Fast-degrading elastomer enables rapid remodeling of a cell-free synthetic graft into a neoartery. Nat Med 2012;18:1148-53.
8. Wystrychowski W, Cierpka L, Zagalski K, Garrido S, Dusserre N, Radochonski S, et al. Case study: first implantation of a frozen, devitalized tissue-engineered vascular graft for urgent hemodialysis access. J Vasc Access 2011;12:67-70.
9. Lawson JH, Glickman MH, Ilzecki M, Jakimowicz T, Jaroszynski A, Peden EK, et al. Bioengineered human acellular vessels for dialysis access in patients with end-stage renal disease: two phase 2 single-arm trials. Lancet 2016;387:2026-34.
10. Wystrychowski W, McAllister TN, Zagalski K, Dusserre N, Cierpka L, L'Heureux N. First human use of an allogeneic tissue-engineered vascular graft for hemodialysis access. J Vasc Surg 2014;60:1353-7.
11. Matsushita H, Inoue T, Abdollahi S, Yeung E, Ong CS, Lui C, et al. Corrugated nanofiber tissue-engineered vascular graft to prevent kinking for arteriovenous shunts in an ovine model. JVS Vasc Sci 2020;1:100-8.
12. Ong CS, Fukunishi T, Liu RH, Nelson K, Zhang H, Wieczorek E, et al. Bilateral arteriovenous shunts as a method for evaluating tissue-engineered vascular grafts in large animal models. Tissue Eng C Methods 2017;23:728-35.
13. Zhou M, Qiao W, Liu Z, Shang T, Qiao T, Mao C, et al. Development and in vivo evaluation of small-diameter vascular grafts engineered by outgrowth endothelial cells and electrospun chitosan/poly(ε-caprolactone) nanofibrous scaffolds. Tissue Eng A 2014;20:79-91.
14. Farber A, Tan T-W, Hu B, Dember LM, Beck GJ, Dixon BS, et al. The effect of location and configuration on forearm and upper arm hemodialysis arteriovenous grafts. J Vasc Surg 2015;62:1258-65.
15. Rui HL, Chin SO, Takuma F, Kingsfield O, Narutoshi H. Review of vascular graft studies in large animal models. Tissue Eng B Rev 2018;24:133-43.
16. Ju YM, Choi JS, Atala A, Yoo JJ, Lee SJ. Bilayered scaffold for engineering cellularized blood vessels. Biomaterials 2010;31:4313-21.
17. Park S, Kim J, Lee M-K, Park C, Jung H-D, Kim H-E, et al. Fabrication of strong, bioactive vascular grafts with PCL/collagen and PCL/silica bilayers for small-diameter vascular applications. Materials Design 2019;181:108079.
18. van Uden S, Vanerio N, Catto V, Bonandrini B, Tironi M, Figliuzzi M, et al. A novel hybrid silk-fibroin/polyurethane three-layered vascular graft: towards in situ tissue-engineered vascular accesses for haemodialysis. Biomed Mater 2019;14:025007.
19. Atlan M, Simon-Yarza T, Ino JM, Hunsinger V, Corté L, Ou P, et al. Design, characterization and in vivo performance of synthetic 2 mm-diameter vessel grafts made of PVA-gelatin blends. Sci Rep 2018;8:7417.
20. Tara S, Kurobe H, Rocco KA, Maxfield MW, Best CA, Yi T, et al. Well-organized neointima of large-pore poly(L-lactic acid) vascular graft coated with poly(L-lactic-co-epsilon-caprolactone) prevents calcific deposition compared to small-pore electrospun poly(L-lactic acid) graft in a mouse aortic implantation model. Atherosclerosis 2014;237:684-91.
21. Spadaccio C, Nappi F, De Marco F, Sedati P, Sutherland FWH, Chello M, et al. Preliminary in vivo evaluation of a hybrid armored vascular graft combining electrospinning and additive manufacturing techniques. Drug Target Insights 2016;10(Suppl 1):1-7.
22. Shi J, Chen S, Wang L, Zhang X, Gao J, Jiang L, et al. Rapid endothelialization and controlled smooth muscle regeneration by electrospun heparin-loaded polycaprolactone/gelatin hybrid vascular grafts. J Biomed Mater Res B Appl Biomater 2019;107:2040-9.
23. Huang R, Gao X, Wang J, Chen H, Tong C, Tan Y, et al. Triple-layer vascular grafts fabricated by combined E-Jet 3D printing and electrospinning. Ann Biomed Eng 2018;46:1254-66.
24. Izhar U, Schwalb H, Borman JB, Hellener GR, Hotoveli-Salomon A, Marom G, et al. Novel synthetic selectively degradable vascular prostheses: a preliminary implantation study. J Surg Res 2001;95:152-60.

25. Lu G, Cui S-J, Geng X, Ye L, Chen B, Feng Z-G, et al. Design and preparation of polyurethane-collagen/heparin-conjugated polycaprolactone double-layer bionic small-diameter vascular graft and its preliminary animal tests. Chin Med J (Engl) 2013;126:1310-6.
26. Pasklinsky G, Meisner RJ, Labropoulos N, Leon L, Gasparis AP, Landau D, et al. Management of true aneurysms of hemodialysis access fistulas. J Vasc Surg 2011;53:1291-7.
27. Valenti D, Mistry H, Stephenson M. A novel classification system for autogenous arteriovenous fistula aneurysms in renal access patients. Vasc Endovasc Surg 2014;48:491-6.
28. Longo GM, Xiong W, Greiner TC, Zhao Y, Fiotti N, Baxter BT. Matrix metalloproteinases 2 and 9 work in concert to produce aortic aneurysms. J Clin Invest 2002;110:625-32.
29. Wilson WRW, Anderton M, Schwalbe EC, Jones JL, Furness PN, Bell PRF, et al. Matrix metalloproteinase-8 and -9 are increased at the site of abdominal aortic aneurysm rupture. Circulation 2006;113:438-45.
30. Longo GM, Buda SJ, Fiotta N, Xiong W, Griener T, Shapiro S, et al. MMP-12 has a role in abdominal aortic aneurysms in mice. Surgery 2005;137:457-62.
31. Tara S, Kurobe H, Maxfield MW, Rocco KA, Yi T, Naito Y, et al. Evaluation of remodeling process in small-diameter cell-free tissue-engineered arterial graft. J Vasc Surg 2015;62:734-43.
32. Wu J, Hu C, Tang Z, Yu Q, Liu X, Chen H. Tissue-engineered vascular grafts: balance of the four major requirements. Colloid Interface Sci Commun 2018;23:34-44.
33. Sugiura T, Tara S, Nakayama H, Yi T, Lee YU, Shoji T, et al. Fast-degrading bioresorbable arterial vascular graft with high cellular infiltration inhibits calcification of the graft. J Vasc Surg 2017;66:243-50.
34. Ozawa T, Mickle DAG, Weisel RD, Koyama N, Wong H, Ozawa S, et al. Histologic changes of nonbiodegradable and biodegradable biomaterials used to repair right ventricular heart defects in rats. J Thorac Cardiovasc Surg 2002;124:1157-64.
35. Rotmans JI, Velema E, Verhagen HJM, Blankensteijn JD, Kastelein JJP, de Kleijn DPV, et al. Rapid, arteriovenous graft failure due to intimal hyperplasia: a porcine, bilateral, carotid arteriovenous graft model. J Surg Res 2003;113:161-71.
36. Hansson GK, Holm J, Holm S, Fotev Z, Hedrich HJ, Fingerle J. T lymphocytes inhibit the vascular response to injury. Proc Natl Acad Sci U S A 1991;88:10530-4.
37. Robertson A-KL, Hansson GK. T cells in atherogenesis: for better or for worse? Arterioscler Thromb Vasc Biol 2006;26:2421-32.

Submitted Jul 24, 2021; accepted Jan 25, 2022.